Journal of Electroceramics, 9, 111–116, 2002

Processing Effects on the Microstructure and Dielectric Properties of Barium Strontium Titanate (BST) Ceramics

B. SU,* J.E. HOLMES, B.L. CHENG & T.W. BUTTON

IRC in Materials Processing, School of Engineering, University of Birmingham, Edgbaston, Birmingham B15 2TT, UK

Submitted February 1, 2002; Revised July 16, 2002; Accepted October 17, 2002

Abstract. Barium Strontium Titanate (BST) ferroelectric thick films have been investigated as potential candidates for use in frequency agile microwave circuit devices. Powder processing techniques such as screen-printing have been used to make BST thick films. However, due to the interactions between the BST and substrates such as alumina, the sintering temperatures for the BST thick films are limited and the resultant films are difficult to achieve full densification. In this paper, the effects of different powder processing conditions (calcination, sintering temperature and time) on the sintering behaviour and dielectric properties of the BST ceramics have been investigated. The dielectric behaviour of the ceramics has been correlated with composition and microstructural features such as chemical homogeneity, grain size and domain wall movements.

Keywords: BST, calcination, sintering, microstructure, dielectric properties

Introduction

Ferroelectric BST ceramics have shown tuneable dielectric properties and low dielectric losses at room temperature and microwave frequencies, which makes them attractive materials for applications in frequency agile microwave circuit devices [1]. BST thick films have recently been investigated as candidates for such applications because of the potential benefits of low fabrication cost together with dielectric properties comparable with their ceramic and thin films forms [2–4]. Conventional powder processing such as screen printing have been used to fabricate BST thick films with thickness from 10 to 50 μm on alumina substrates. Thick films are expected to possess similar dielectric properties to their bulk analogues while only need relatively small DC bias voltages to achieve large tunability. However, previous investigation showed severe interactions between the BST thick films and commonly used low dielectric substrate materials such as alumina [5]. The sintering temperatures for the BST films are significantly restricted and the films are not fully densified. Even though, the BST films still show significant tunabilities up to 35% at a DC bias field of 2 kV/cm [6]. Therefore, it is important to understand the processing-structure-properties relationships of the bulk BST ceramics and thick films at different processing conditions, especially, at lower sintering temperatures.

The dielectric properties of the BST compositions in the form of both ceramics [7–12] and single crystals [13] have been investigated since mid 1940's. However, much attention has been paid to the compositional effects on the Curie temperature and dielectric properties of BST ceramics [14–16]. Only few studies have been reported of the microstructural aspects relating processing conditions to the dielectric properties [12, 17, 18] and, in particular, the dielectric dissipation [19]. The objective of this paper is, therefore, to investigate the effects of processing conditions during BST powder synthesis and subsequent sintering on the microstructure and dielectric properties of BST ceramics. Dielectric spectra of the BST ceramics with temperatures and frequencies have been measured and the results are discussed with respect to their composition, grain sizes and domain wall movements.

*To whom all correspondence should be addressed.

Experimental

$Ba_{0.6}Sr_{0.4}TiO_3$ powders were synthesised from stoichiometric powders of titania (>99.9% Thermometrics), barium carbonate (99%, Fluka) and strontium carbonate (99%, Fluka) using a solid-state reaction route. After mixing and ball milling in acetone with zirconia media for 24 h, the powders were calcined at temperatures from 900 to 1150°C with calcination time from 20 min to 20 h. The calcined powders were re-milled with binder and dry pressed at 100 MPa. The pellets were then sintered in air at temperatures from 1300 to 1450°C for 2 h using a heating rate of 5°C/min.

A Philip X'pert X-ray diffraction was used to characterise the crystallisation of the BST powders and sintered ceramics. Particle sizes and size distributions of the calcined powders were characterised using a Coulter LS130 particle size analyser. The density and shrinkage were calculated from the measured weights and dimensions. The sintering behaviour in air was monitored via a Netzsch differential dilatometer using a sapphire reference and a heating rate of 10°C/min. The microstructure of the BST ceramics were characterised using a Philips XL30 scanning electron microscopy. The dielectric properties were measured using a HP 4194A impedance analyser at an applied voltage of 500 mV and connected to an environmental chamber to control the measurement temperature. Silver paint was used as an electrode material. The measurement frequencies were varied from 10^2 to 10^6 Hz in the temperatures range from −70 to 70°C.

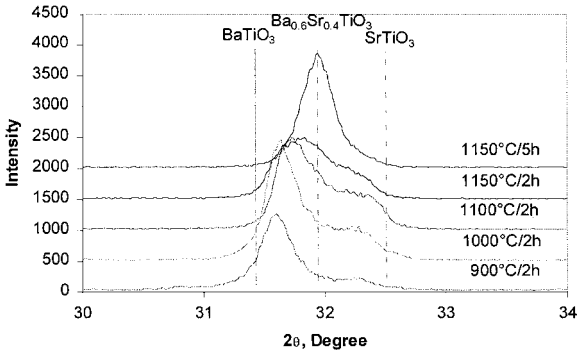

Fig. 1. XRD traces showing the calcination temperatures and times on the phase formation of $Ba_{0.6}Sr_{0.4}TiO_3$ powders.

Results and Discussion

The XRD results in the range of $2\theta = 30$–34° for powders calcined at different temperatures and time are shown in Fig. 1. The expected positions of the [110] peak for $Ba_{0.6}Sr_{0.4}TiO_3$, $BaTiO_3$ and $SrTiO_3$ are also marked. Biphasic BST solid solution was formed during calcination at temperatures below 1150°C. As the

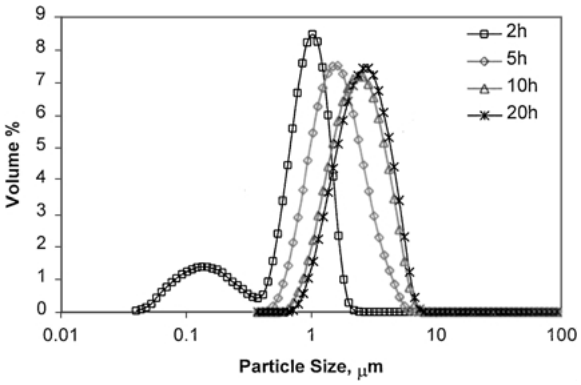

Fig. 2. Particle size distributions of $Ba_{0.6}Sr_{0.4}TiO_3$ powders calcined at 1150°C for 2 h, 5 h, 10 h and 20 h.

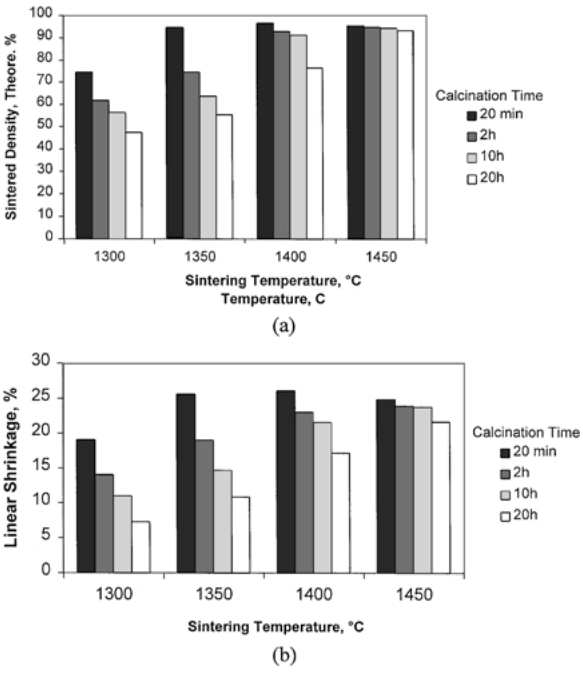

Fig. 3. The effect of sintering temperature on sintered density (a) and linear shrinkage (b) for $Ba_{0.6}Sr_{0.4}TiO_3$ powders calcined for 20 min, 2 h, 10 h and 20 h.

temperature increases, the inter-diffusion of $BaTiO_3$ and $SrTiO_3$ increases as the two peaks moving together. But the single phase BST solid solution was not formed until the powders were calcined at 1150°C for more than 5 h. Therefore, prolonged calcination time at 1150°C was need to ensure single phase BST solid solution formation. Shorter calcination times and lower calcination temperatures may result in chemical inhomogeneity within the calcined powders.

The effect of calcination time at the calcination temperature of 1150°C on the particle size and distributions is shown in Fig. 2. The particle size is increased with the calcination time. The measured mean particle sizes of the BST powders are 0.8, 1.6, 2.4 and 2.7 μm for the calcination times of 2 h, 5 h, 10 h and 20 h, respectively. The increase in particle size of BST powders will affect their respective sintering behaviour.

The effect of sintering temperature on sintered density and linear shrinkage for BST ceramics from powders calcined at 1150°C for different times is shown in Fig. 3. For the same sintering conditions, BST powders

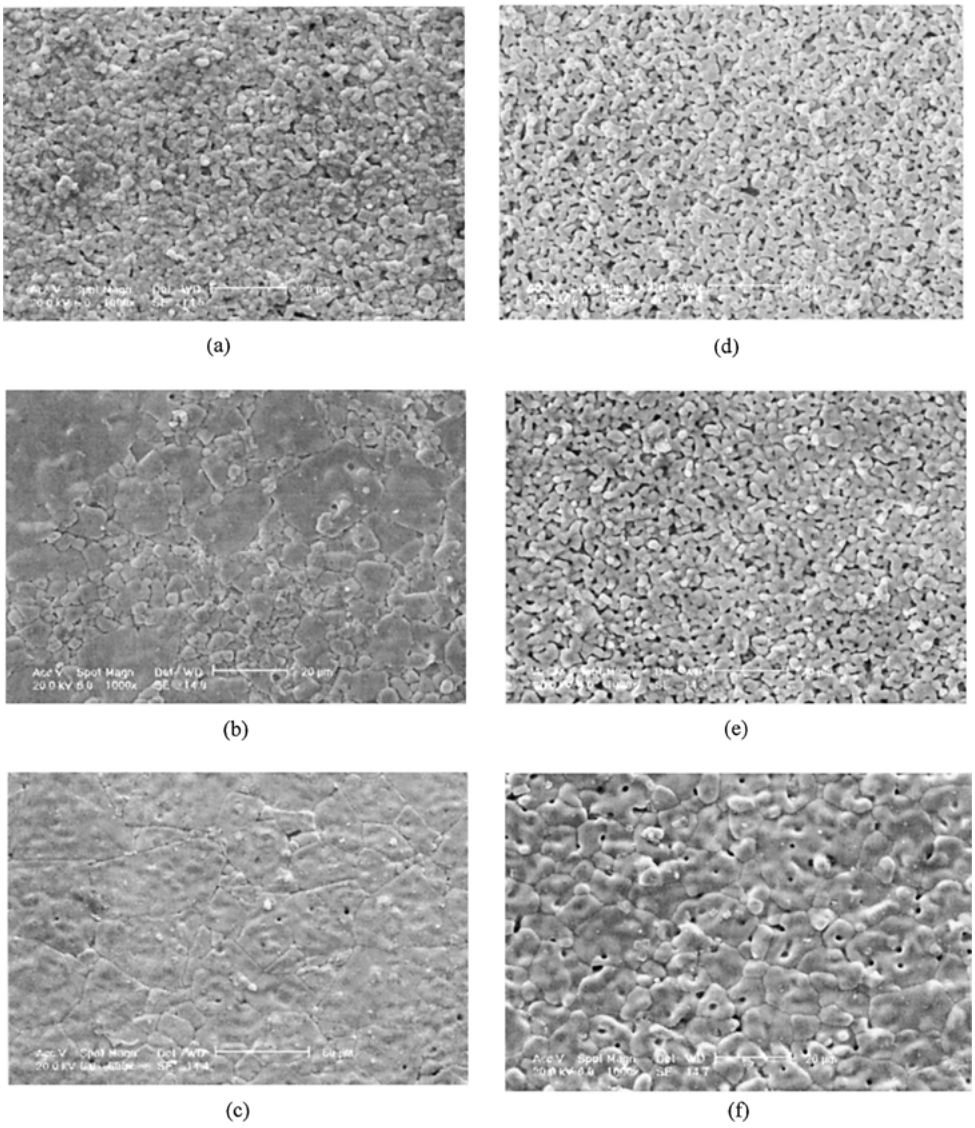

Fig. 4. SEM micrographs of the $Ba_{0.6}Sr_{0.4}TiO_3$ ceramics produced from powders calcined at 1150°C for 20 min and sintered at (a) 1350; (b) 1400; and (c) 1450°C for 2 h, and powders calcined at 1150°C for 20 h and sintered at (d) 1350; (e) 1400; and (f) 1450°C for 2 h, respectively.

calcined for shorter times have noticeably higher sintered densities and larger sintering shrinkages.

The effects of calcination and sintering conditions on the microstructure of the BST ceramics are shown in Fig. 4. The SEM results show that for all sintering temperatures ceramics produced from the powders calcined for 20 h have a lower sintered density than those produced from the powders calcined only for 20 min. In addition, for the ceramics sintered at temperatures of 1400 and 1450°C, the samples produced from the powders calcined for 20 h have a much more homogenous grain size distribution than those produced from powders calcined for 20 min, where some abnormally large grains are observed.

It was noted above that for the finer particle size distributions of the powders calcined for the shorter times would give rise to differences in sintering behaviour. In addition, the XRD data indicated that the powder calcined at 1150°C for less than 2 h may be chemically inhomogeneous which could cause titania-rich phases in the microstructure. Kollar et al. [20] reported the formation of a polytitanate phase ($Ba_6Ti_{17}O_{40}$) during sintering in the system $BaTiO_3$-$SrTiO_3$ as a consequence of preferential diffusion of Ba^{2+} ions into $SrTiO_3$. This is also confirmed in our XRD result. As can be seen in Fig. 5, polytitanates residues were detected in sintered BST ceramics from the powder calcined for only 20 min. The polytitanate formed a low-temperature (ca. 1320°C) eutectic liquid with $BaTiO_3$ [21] which was postulated to be the cause of abnormal grain growth observed in this system. Similar results have been reported for non-stoichiometric $BaTiO_3$ ceramics [22]. The combination of these effects could be responsible for the different microstructures observed here.

Shrinkage rate curves for different BST powder compacts also show different sintering behaviour

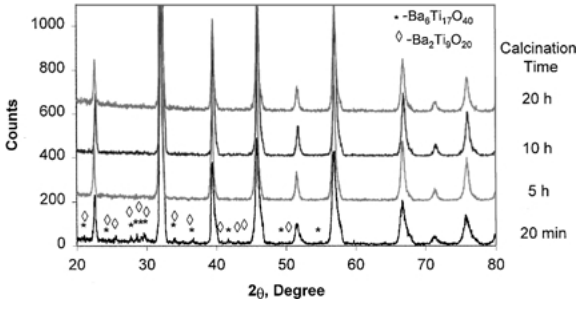

Fig. 5. XRD patterns of sintered BST ceramics from powders calcined at 1150°C for different time.

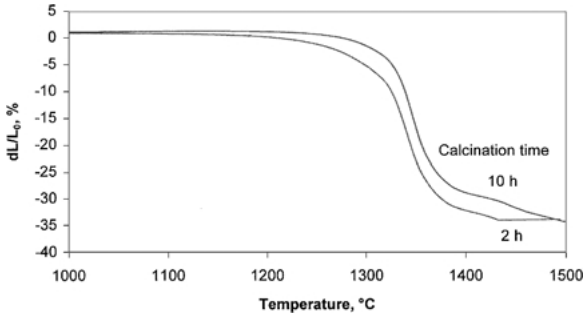

Fig. 6. Sintering shrinkage cueves of green compacts of BST powders calcined at 1150°C for 2 h and 10 h, respectively.

(Fig. 6). The onset temperatures and maximum shrinkage rates shift to slightly lower temperatures for BST powder calcined at 1150°C for 2 h compared to powder calcined for 10 h, which may be attributed to the combined effects of smaller particle sizes as shown in Fig. 2 and possible liquid phase sintering of the titania-rich phase arisen from the incomplete calcination as discussed before.

The dielectric properties corresponding to the BST ceramics illustrated in Fig. 4 are shown in Figs. 7 and 8, respectively. It can be seen that the dielectric dissipation in the paraelectric (PE) region is less than 10^{-3} (the Curie temperature for the $Ba_{0.6}Sr_{0.4}TiO_3$ in this work is ca. 6°C). The height of the peak of dissipation in the ferroelectric (FE) region decreases with increasing of sintering temperature for samples from both powders. This corresponds to a reduced loss as sintered density increases. In general, the peak loss value is less than 0.015 when the sintered density is more than 90%. The broad relaxation shoulder in the FE region is thought to be due to the losses from domain wall movement, and this would be expected to be dependent on the grain size [23]. The relaxation peak is observed to decrease with increasing sintered densities as shown in Fig. 7. Relaxation peaks have been observed in the BST ceramics with grain sizes larger than 1 μm, which could be the result of the interactions between different domain wall configurations and the diffusion of oxygen vacancies in the domains. Grain boundary conditions will also influence the relaxation process. The lower sintered density and thus higher porosity in the BST ceramics will result in a decreased clamping effect from the grain boundaries and an increased nucleation rate of new domain walls within the relatively loosely connected grains [24]. Both of these effects will contribute to the increased dissipation of BST ceramics. This may

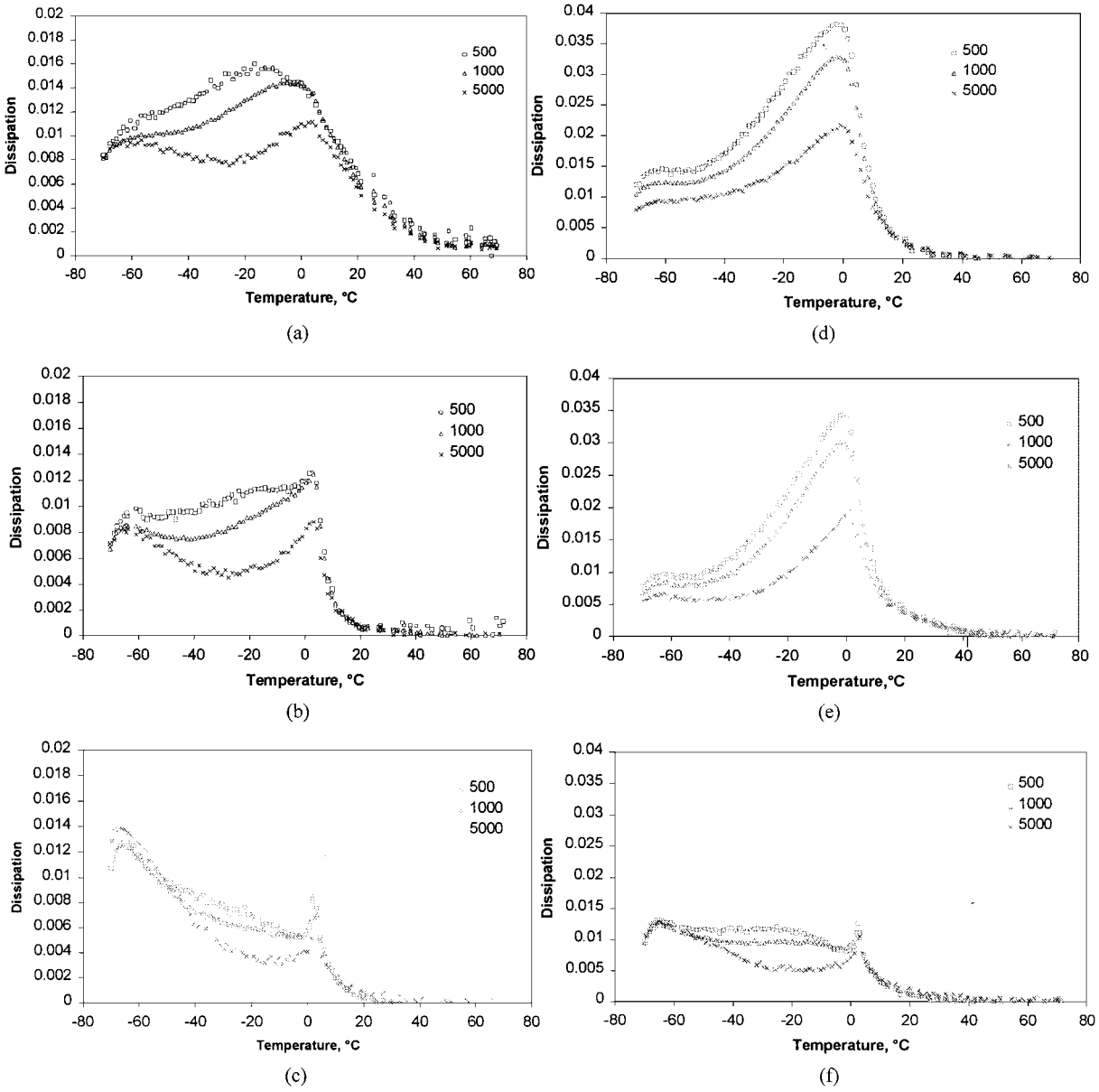

Fig. 7. Dielectric dissipation measured at frequency of 500, 1000 and 5000 Hz for the $Ba_{0.6}Sr_{0.4}TiO_3$ ceramics produced from powders calcined at 1150°C for 20 min and sintered at (a) 1350; (b) 1400; and (c) 1450°C for 2 h, and powders calcined at 1150°C for 20 h and sintered at (d) 1350; (e) 1400; and (f) 1450°C for 2 h, respectively. For clarity, curves at other frequencies have been omitted.

explain why the loss value is doubled if the sintered density is less than 80% as in the case for samples shown in Fig. 4(d) and (e).

The permittivity of the BST ceramics increases with the sintering temperature as shown in Fig. 8. For ceramics sintered at the same temperature, a broader permittivity maximum near the T_c has been observed for the BST ceramics produced from powders calcined at 1150°C for 20 h. The diffuseness is attributed to their smaller grain size [25] due to the absence of abnormal grain growth which occurred in ceramics from powders calcined for 20 min.

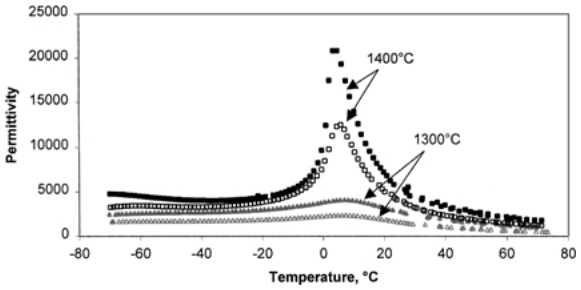

Fig. 8. Temperature dependence of the permittivity of $Ba_{0.6}Sr_{0.4}TiO_3$ ceramics sintered at 1300 and 1400°C, produced from powders calcined at 1150°C for 20 min (solid) and 20 h (hollow), respectively.

Conclusions

Calcination and sintering conditions have significant effects on the microstructure and dielectric properties, in particular, the dissipation of BST ceramics produced via an oxide-carbonate route. The calcination conditions should be at least 1150°C for 5 h to obtain single phase, compositionally homogeneous BST powders. Incomplete calcination results in enhanced sintering and abnormal grain growth. However, prolonged calcination time increases the particle size and decreases the sintered density of the ceramics.

The dielectric dissipation generally decreases as the sintered density of ceramics increases. This is thought to be due to a grain boundary pining effect which hinders the movement of domain walls in the FE region. The peak in the dielectric loss near T_c in the FE region may also result from the increased nucleation rate of domain walls arising from a decreased clamping effect for the less dense BST ceramics.

The dielectric permittivity generally increases as the sintering temperature and sintered density increase. The broader maximum near the T_c for ceramics produced from powders calcined at longer times may be attributed to the diffuseness caused by smaller grain size.

Acknowledgments

The authors wish to thank EPSRC for the financial support and G. Dolman for dilatometry measurements.

References

1. J.B.L. Rao, D.P. Patel, V. Krichevsky, L.C. Sengupta, L. Chiu, X. Zhang, Y. Zhu, S. Stowell, S. Sengupta, and A. Moffat, *Integrated Ferroelectrics*, **24**, 309 (1999).
2. B. Su and T.W. Button, *J. Euro. Ceram. Soc.*, **21**, 2641 (2001).
3. C. Weil, P. Wang, H. Downar, J. Wenger, and R. Jakoby, *Frequenz*, **54** (11/12), 250 (2000).
4. F. Zimmermann, M. Voigts, C. Weil, R. Jakoby, P. Wang, W. Menesklou, and E. Ivers-Tiffee, *J. Euro. Ceram. Soc.*, **21**, 2019 (2001).
5. B. Su and T.W. Button, *J. Euro. Ceram. Soc.*, **21**, 2777 (2001).
6. B. Su, J.E. Holmes, C. Meggs, and T.W. Button, to be presented at MMA 2002, 1–3 Sept., 2002, York, UK.
7. W. Jackson and W. Reddish, *Nature*, **156**, 717 (1945).
8. S. Roberts, *Phys. Rev.*, **71**, 890 (1947).
9. L. Davis Jr. and L.G. Rubin, *J. Appl. Phys.*, **24**, 1195 (1953).
10. D. Barb, E. Barbulescu, and A. Barbulescu, *Phys. Stat. Sol.* (a), **74**, 79 (1982).
11. J.W. Liou and B.S. Chiou, *Mater. Chem. Phy.*, **51**, 59 (1997).
12. S.M. Rhim, H. Bak, S. Hong, and O.K. Kim, *J. Am. Ceram. Soc.*, **83**, 3009 (2000).
13. L. Benguigui and K. Bethe, *J. Appl. Phys.*, **47**, 2787 (1976).
14. U. Syamaprasad, R.K. Galgali, and B.C. Mohanty, *Mater. Lett.*, **7**(5/6), 197 (1988).
15. L. Zhou, P.M. Vilarinho, and J.L. Baptista, *J. Euro. Ceram. Soc.*, **19**, 2015 (1999).
16. S.B. Herner, F.A. Selmi, V.V. Varadan, and V.K. Varadan, *Mater. Lett.*, **15**, 317 (1993).
17. P.C. Osbond, N.I. Payne, N.M. Shorrocks, R.W. Whatmore, and F.W. Ainger, *in ISAF'86, Proceedings of the Sixth IEEE International Symposium on Applications of Ferroelectrics*, (IEEE, New York, USA, 1986), p. 738.
18. U. Kumar, S.F. Wang, S. Varanasi, and J.P. Dougherty, *in ISAF'92, Proceedings of the Eighth IEEE International Symposium on Applications of Ferroelectrics*, (IEEE, New York, NY, USA, 1992), p. 55.
19. L. Zhang, W.L. Zhang, C.L. Wang, P.L. Zhang, and Y.G. Wang, *Solid State Communications*, **107**(12), 769 (1998).
20. D. Kollar, M. Trontelj, and Z. Stadler, *J. Am. Ceram. Soc.*, **65**(10), 470 (1982).
21. D.E. Rase and R. Roy, *J. Am. Ceram. Soc.*, **38**, 102 (1955).
22. P.R. Rios, T. Yamamoto, T. Kondo, and T. Sakuma, *Acta Mater.*, **46**(5), 1617 (1998).
23. B.L. Cheng, B. Su, J.E. Holmes, T.W. Button, M. Gabbay, and G. Fantozzi, *J. Mater. Sci.*, submitted.
24. Y.N. Huang, Y.N. Wang, and H.M. Shen, *Phy. Rev.* B, **46**, 3290, (1992).
25. L. Zhang, W.L. Zhong, C.L. Wang, Y.P. Peng, and Y.G. Wang, *Euro. Phys. J.* B, **11**, 565 (1999).